IV.A.6 Effects and Mechanisms of Mechanical Activation on Hydrogen Sorption/Desorption of Nanoscale Lithium Nitrides and Lithium Borohydrides

Leon L. Shaw (Primary Contact), Tippawan Markmaitree, William Osborn, Xuefei Wan, Kyle Crosby
University of Connecticut
97 N. Eagleville Road
Storrs, CT 06269
Phone: (860) 486-2592; Fax: (860) 486-4745
E-mail: leon.shaw@uconn.edu

DOE Technology Development Manager: Ned Stetson
Phone: (202) 586-9995; Fax: (202) 586-9811
E-mail: Ned.Stetson@ee.doe.gov

DOE Project Officer: Katie Randolph
Phone: (303) 275-4901; Fax: (303) 275-4753
E-mail: Katie.Randolph@go.doe.gov

Contract Number: DE-FC36-05GO15008

Subcontractors:
Z. Gary Yang, Jianzhi Hu, Ja Hun Kwak
Materials Division, Pacific Northwest National Laboratory
Richland, WA

Start Date: December 9, 2004
Projected End Date: December 8, 2009

Objectives

- Investigate the effects and mechanisms of mechanical activation on hydrogen sorption/desorption behavior of Li_3N- and $LiBH_4$-based materials.
- Develop a novel, mechanically activated, nanoscale Li_3N- or $LiBH_4$-based material that is able to store and release ~10 wt% hydrogen at temperatures below 100°C with a plateau hydrogen pressure of less than 10 bar.

Technical Barriers

This project addresses the following technical barriers from the Storage section of the Hydrogen, Fuel Cells and Infrastructure Technologies Program Multi-Year Research, Development and Demonstration Plan:

(A) System Weight and Volume

(E) Charging/Discharging Rates

Technical Targets

This project is to develop a fundamental understanding of effects and mechanisms of mechanical activation on hydrogen storage capacity and sorption/desorption kinetics of nanoscale Li_3N- and $LiBH_4$-based materials. Insights gained from these studies will be applied to producing a novel, mechanically activated, nanoscale Li_3N- or $LiBH_4$-based material that meets the following DOE 2010 hydrogen storage targets:

- Cost: $4/kWh net
- System gravimetric capacity: 1.5 kWh/kg
- System volumetric capacity: 0.9 kWh/L
- Charging/discharging rates: 4.2 min for 5 kg

Progress towards meeting the DOE on-board hydrogen storage targets made up to Fiscal Year 2009 is summarized in Table 1.

TABLE 1. Progress Towards Meeting the DOE On-Board Hydrogen Storage Targets

Storage Parameter	Units	2010 System Target	FY09 Material Status
Specific Energy	kWh/kg (kg H_2/kg system)	1.5 (0.045)	3.17 at 265°C (0.095 at 265°C)
Energy Density	kWh/L (kg H_2/L system)	0.9 (0.028)	2.54 at 265°C (0.079 at 265°C)
Charging/ Discharging Rate (system fill time for 5 kg)	min	4.2	300 at 265°C

Accomplishments

- Developed a two-step ball milling procedure to improve the solid-state hydriding and dehydriding kinetics of $LiBH_4 + MgH_2$ systems.
- Demonstrated the solid-state hydriding and dehydriding of $LiBH_4 + MgH_2$ systems with 9.5 wt% hydrogen uptake and 4.5 wt% hydrogen release at 265°C. These are the best hydriding and dehydriding properties for the $LiBH_4 + MgH_2$ system ever reported in the open literature.
- Identified the solid-state hydriding mechanism of the $LiBH_4 + MgH_2$ system and established a partial ion-exchange model to guide the improvement of the diffusion-controlled hydriding reaction.
- Achieved the hydrogen release from nanoscale $LiBH_4$ confined within carbon aerogels (CAs) at temperatures as low as 80°C with the peak

releasing temperature at 165°C and the completion temperature at 275°C. These H_2 release temperatures are the lowest ever reported in the open literature for $LiBH_4$. More importantly, these hydrogen release behaviors approach the DOE target – releasing H_2 below 100°C!

- Demonstrated that the hydrogen released from CA-confined $LiBH_4$ contained no borane – an impurity that is likely to poison proton exchange membrane (PEM) fuel cells.

Introduction

A key component for the hydrogen economy is fuel cell vehicles which, in turn, depend critically upon advanced hydrogen storage materials. The challenge is to develop a storage material that simultaneously satisfies three competitive requirements: (i) high hydrogen density, (ii) reversibility of hydrogen release/uptake cycle near the ambient temperature and pressure, and (iii) fast release/uptake kinetics. This project is aimed at investigation and development of such hydrogen storage materials with capabilities to reversibly uptake and release hydrogen near the ambient temperature and pressure.

Approach

To achieve the project objectives, we have employed nano-engineering and mechanical activation approaches to develop hydrogen storage materials that simultaneously satisfy the three requirements mentioned above. In the last year, we switched our focus from ($LiNH_2$+LiH)-based systems to ($LiBH_4$+MgH_2)-based systems because the latter have a theoretical storage capacity of 11.5 wt% H_2, while the former only have a theoretical storage capacity of 6.5 wt% H_2. It was shown previously that hydriding and dehydriding processes of both systems were diffusion controlled [1,2]. Therefore, nano-engineering and mechanical activation approaches are pursued to reduce the hydride particle sizes, increase their surface areas, and mix the reactants at the nanoscale – all of which will enable rapid sorption and desorption of hydrogen molecules on the solid surface, provide large interfacial area for reactions between solid hydrides, and reduce the diffusion distance of hydrogen within the solids.

Results

Figure 1 shows the hydriding performance of a 2LiH+MgB_2 mixture processed with a two-step ball milling procedure. Note that this two-step ball milled mixture exhibits hydrogen uptake of 9.5 wt% at 265°C. This is the best hydriding property at 265°C ever

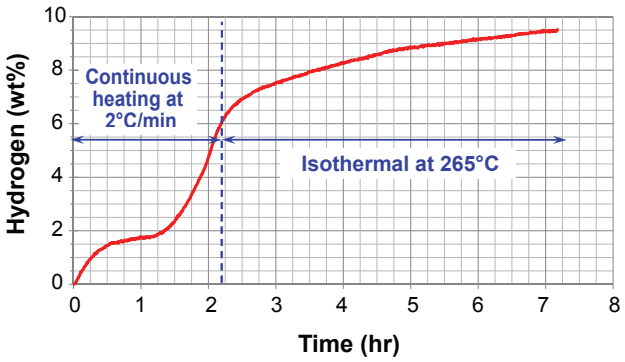

FIGURE 1. Hydrogenation behavior of a two-step ball milled 2LiH + MgB_2 mixture. The two-step ball milling entails (a) ball milling at room temperature for 120 h and then (b) ball milling at liquid nitrogen temperature for 1 h with the addition of 15 vol% graphite. The hydrogenation was conducted under a hydrogen pressure of 90 bar with the heating condition indicated.

reported in the open literature for $LiBH_4$+MgH_2 systems. The overall reaction corresponding to the hydriding reaction of the 2LiH+MgB_2 mixture is [3]

$$2\,LiBH_4 + MgH_2 \leftrightarrow 2\,LiH + MgB_2 + 4\,H_2 \quad (1)$$

The superior hydriding performance shown in Figure 1 results from the two-step ball milling procedure which entails ball milling the 2LiH+MgB_2 mixture at room temperature for 120 h and then at liquid nitrogen temperature for 1 h with addition of 15 vol% graphite at the second-step milling. The first-step ball milling reduces the grain sizes of LiH and MgB_2 to 7.5 and 6.8 nm, respectively, and mixes them uniformly within nanostructured particles with the average size of 260 nm [2]. This ball milled mixture can uptake 8.3 wt% H_2 at 265°C because of the enhanced diffusion coefficients due to the presence of large grain boundary and interfacial areas within the nanostructured particles [2]. The second-step ball milling, although in a relatively short duration, introduces nano-graphite to the grain boundaries and interfaces within nanostructured particles because of frequent fracture and cold welding of particles during ball milling. The presence of the trapped nano-graphite leads to more open structures at the grain boundaries and interfaces, thereby increasing the diffusion rates of H, Mg, Li and B all of which are needed for the hydriding reaction. It should be pointed out that two-step ball milling is necessary to achieve this superior performance because long-time ball milling with the addition of graphite results in reactions between LiH and graphite during ball milling and degrades the hydriding performance rather than improving it (not shown here).

The two-step ball milling procedure also improves the dehydriding properties. As shown in Figure 2, the one-step ball milled mixture can only release 2.0 wt% H_2 at 265°C, whereas the two-step ball milled counterpart

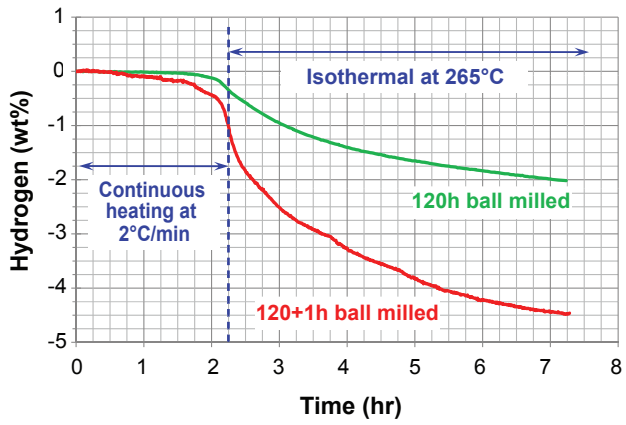

FIGURE 2. A comparison of the dehydrogenation behavior between a two-step ball milled 2LiH + MgB_2 mixture (i.e., 120+1 h sample) and a one-step ball milled mixture (120 h sample). Both ball milled samples were first hydrogenated under the condition shown in Figure 1. After the hydrogenation, the dehydrogenation was conducted under an evacuated condition (~0.03 bar) with the heating condition indicated.

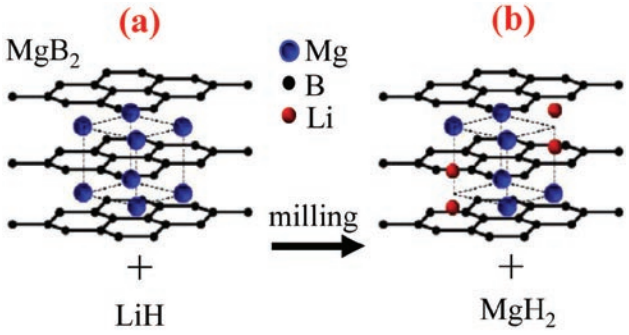

FIGURE 3. Proposed structure changes of the LiH + MgB_2 mixture: (a) before and (b) after long-time ball milling.

can release 4.5 wt% H_2, exhibiting a 125% improvement over the one-step ball milled mixture. The improvement is attributed to the presence of the trapped nano-graphite within nanostructured particles. Note that releasing 4.5 wt% H_2 requires the participation of a large amount of $LiBH_4$ and all of MgH_2 in the dehydriding process. It has been shown previously that $LiBH_4$ and MgH_2 do not react directly in the dehydriding process [2-6]. Instead, MgH_2 decomposes into Mg and H_2 first and then the newly formed Mg and H_2 react with $LiBH_4$ to produce LiH, MgB_2 and H_2. It is proposed that the trapped nano-graphite in the two-step ball milled mixture enhances the diffusion rate of Mg at grain boundaries and interfaces, thereby accelerating the reaction among Mg, $LiBH_4$ and H_2 to produce LiH, MgB_2 and H_2 with higher rates.

Figure 3 shows a model of the molecular interaction between LiH and MgB_2 during long-time ball milling. This model is proposed based on the detailed nuclear magnetic resonance (NMR) analysis [7]. Before ball milling, all the magnesium atoms are located between the boron layers and each is along the central symmetric axis of the boron hexagonal structure (Figure 3a). After long-time ball milling, a significant amount of magnesium sites are exchanged with lithium (Figure 3b) to form a compound with a composition of $(Mg_{1-x}Li_{2x})B_2$ to maintain the charge balance. Each expelled magnesium combines with two protons from LiH to form MgH_2. The formed MgH_2 is located at the immediate surface of the $(Mg_{1-x}Li_{2x})B_2$ structure and in an amorphous state. This partial ion exchange mechanism can be described by

$$2LiH + MgB_2 \xrightarrow[\text{Ball milling}]{} (Mg_{1-x}Li_{2x})B_2 + xMgH_2 + (2-2x)LiH \quad (2)$$

where x is a variable changing from 0 (for MgB_2) to less than 1, depending on the time of ball milling. The model proposed is consistent with the NMR analysis [7], showing that approximately 50% of MgB_2 has been converted to MgH_2 accompanied by only ~1% $LiBH_4$ formation after ball milling at room temperature for 120 h. The model proposed is also consistent with the previous X-ray diffraction (XRD) analysis [2], showing the absence of MgH_2 after 120 h ball milling because of the amorphous state of MgH_2. This model is also in good accordance with the Fourier transform infrared analysis, showing little $LiBH_4$ formation [7]. The formation of the compound $(Mg_{1-x}Li_{2x})B_2$ is likely the key reason for the observed enhancement in the subsequent solid-state hydrogenation [2]. Although the detail of hydrogenation mechanism remains to be studied, one possible reaction pathway is the continued Mg-Li ion exchange within $(Mg_{1-x}Li_{2x})B_2$ and simultaneous hydrogenation of $(Mg_{1-x}Li_{2x})B_2$. It is noted that the extreme case of the continued Mg-Li ion exchange is the formation of the LiB crystal. LiB has been observed experimentally [8]. Furthermore, the first-principles calculations reveal that Li is in the state of Li^+ ion in LiB [9] and stabilizes the hexagonal layers of boron in LiB [10]. Therefore, gradual transition from MgB_2 to LiB through the intermediate $(Mg_{1-x}Li_{2x})B_2$ will involve no change in the hexagonal layers of boron and no charge unbalance. Although pure LiB may not form during the subsequent hydrogenation because of the simultaneous Mg-Li ion exchange and hydrogenation of $(Mg_{1-x}Li_{2x})B_2$, the formation of Li-rich $(Mg_{1-x}Li_{2x})B_2$ compound is expected to facilitate the formation of $LiBH_4$ because the removal of Mg from MgB_2 is necessary for the formation of $LiBH_4$.

Figure 4 shows the H_2 gas profile from nanoscale $LiBH_4$ confined within CAs during a thermogravimetric analysis (TGA). It reveals that CA-confined $LiBH_4$ can release H_2 at temperatures as low as 80°C with the peak releasing temperature at 165°C and the completion temperature at 275°C. These H_2 release temperatures are the lowest ever reported in the open literature for

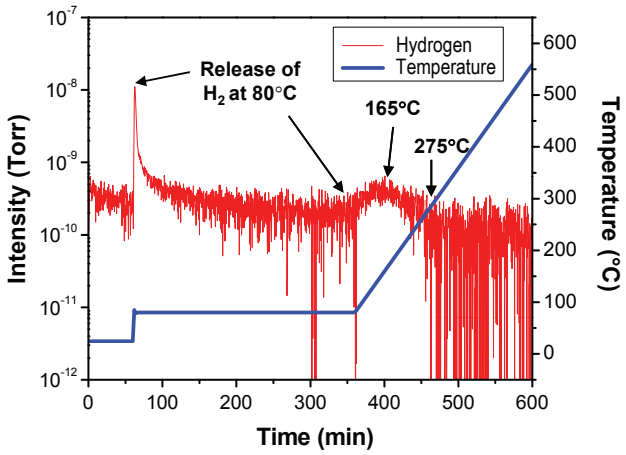

FIGURE 4. The temperature profile during a thermogravimetric (TG) analysis of $LiBH_4$ confined within a CA and the corresponding effluent hydrogen profile measured using an on-line mass spectrometer. The heating condition was: (i) held at room temperature for 60 min, (ii) jumped to 80°C and held for 300 min, and (iii) heated at 2°C/min to 550°C. All the procedures were conducted in an argon-filled glovebox with flowing argon in the TG chamber.

$LiBH_4$. More importantly, this dehydriding property approaches the DOE target – releasing H_2 below 100°C! Furthermore, no emission of borane, B_2H_6 – an impurity that is likely to poison PEM fuel cells and frequently found in the hydrogen released from $LiBH_4$ [11], is detected in the entire temperature range (not shown in Figure 4), suggesting that emission of borane can be avoided if hydrogen is released at low temperatures. We believe that the unprecedented enhancement in the dehydriding behavior of $LiBH_4$ shown in Figure 4 is due to the formation of sub-nm particles, which results in a drastically reduced diffusion distance and the associated improvement in the thermodynamic properties. By characterizing CAs before and after infiltration of $LiBH_4$ in a tetrahydrofuran (THF) solution and removing of the THF solvent under vacuum at room temperature for 20 h, we find that the average diameter of the CA-confined $LiBH_4$ particles is ~0.75 nm. It is these sub-nm particles that lead to the unprecedented enhancement in the dehydriding behavior of $LiBH_4$. It should be pointed out that to ensure that the H_2 gas observed in Figure 4 is from $LiBH_4$ only, we have conducted the identical TGA experiments coupled with an on-line mass spectrometer on the CA alone, THF solvent only, and THF-infiltrated CAs. The results indicate that hydrogen is from $LiBH_4$ only.

Conclusions and Future Directions

The successful demonstration of 9.5 wt% hydrogen uptake and 4.5 wt% hydrogen release of $LiBH_4 + MgH_2$ systems in the solid state without any catalysts indicates that nano-engineering and mechanical activation are effective methods in enhancing diffusion-controlled reactions. Therefore, in the remainder of FY 2009, efforts will be focused on exploring the integration of nano-engineering, mechanical activation, and addition of effective transition metals to further increase the diffusion rates and thus reduce the hydrogen uptake and release temperature of $LiBH_4 + MgH_2$ systems.

The unprecedented enhancement in the dehydriding behavior of nanoscale $LiBH_4$ confined within CAs is scientifically and technologically important. Thus, its hydriding and dehydriding reversibility will be investigated in the remainder of FY 2009. Furthermore, the storage capacity of CA-confined $LiBH_4$ will be increased through high loading of $LiBH_4$ in CAs and the relationship between the $LiBH_4$ loading and the kinetics of hydriding and dehydriding processes will be studied in order to provide guidelines for developing high-performance hydrogen storage materials that meet the DOE 2015 targets.

FY 2009 Publications/Presentations

1. W. Osborn, T. Markmaitree, L. Shaw, J.Z. Hu, J.H. Kwak, and Z.G. Yang, "Low Temperature Milling of the $LiNH_2$ + LiH Hydrogen Storage System," *Int. J. Hydrogen Energy*, 34, 4331-4339 (2009).

2. W. Osborn, T. Markmaitree, and L. Shaw, "Long-Term Hydriding and Dehydriding Stability of the Nanoscale $LiNH_2$ + LiH Hydrogen Storage System," *Nanotechnology*, 20, 204028 (2009).

3. J.Z. Hu, J.H. Kwak, Z. Yang, X. Wan, and L. Shaw, "Direct Observation of Ion Exchange in Mechanically Activated LiH+MgB_2 System Using Ultra-High Field Nuclear Magnetic Resonance Spectroscopy," *Appl. Phys. Lett.*, 94, 141905 (2009).

4. W. Osborn, T. Markmaitree, L. Shaw, R. Ren, J.Z. Hu, J.H. Kwak, and Z.G. Yang, "Solid-State Hydrogen Storage: Storage Capacity, Thermodynamics, and Kinetics," *JOM*, 61 [4] 45-51 (2009).

5. X. Wan, T. Markmaitree, W. Osborn, and L. Shaw, "Nanoengineering-Enabled Solid-State Hydrogen Uptake and Release in the $LiBH_4$ plus MgH_2 System," *J. Phys. Chem. C*,112, 18232-18243 (2008).

6. L. Shaw, T. Markmaitree, W. Osborn, X. Wan, K. Crosby, Z.G. Yang, J.Z. Hu, and J.H. Kwak, "Effects and Mechanisms of Mechanical Activation on Hydrogen Sorption/Desorption of Nanoscale Lithium Nitrides," presented at the FreedomCAR and Fuel Hydrogen Storage Technical Team Meeting, Detroit, MI, May 14, 2008.

7. L. Shaw, T. Markmaitree, W. Osborn, X. Wan, K. Crosby, Z.G. Yang, J.Z. Hu, and J.H. Kwak, "Solid-State Hydriding and Dehydriding of $LiBH_4 + MgH_2$ Enabled via Mechanical Activation and Nano-Engineering," presented at the 2009 DOE Hydrogen Program Review, Arlington, VA, May 18–22, 2009.

References

1. L. Shaw, W. Osborn, T. Markmaitree, and X. Wan, "The reaction pathway and rate-limiting step of dehydrogenation of $LiHN_2$ + LiH mixture," J. Power Sources, 177, 500 (2008).

2. X. Wan, T. Markmaitree, W. Osborn, and L. Shaw, "Nanoengineering-enabled solid-state hydrogen uptake and release in the $LiBH_4$ plus MgH_2 system," J. Phys. Chem. C, 112, 18232 (2008).

3. J. Vajo, S. Skeith, and F. Mertens, "Reversible storage of hydrogen in destabilized $LiBH_4$," J. Phys. Chem. B: Lett., 109, 3719 (2005).

4. X.B. Yu, D.M. Grant, and G.S. Walker, "A new dehydrogenation mechanism for reversible multicomponent borohydride systems – the role of Li-Mg alloys," Chem. Commun., 3906-3908 (2006).

5. F.E. Pinkerton, M.S. Meyer, G.P. Meisner, M.P. Balogh, and J.J. Vajo, "Phase boundaries and reversibility of $LiBH_4$/MgH_2 hydrogen storage material," J. Phys. Chem. C, 111, 12881-12885 (2007).

6. T. Nakagawa, T. Ichikawa, N. Hanada, Y. Kojima, and H. Fujii, "Thermal analysis on the Li-Mg-B-H systems," J. Alloys Compd., 446-447, 306 (2007).

7. J.Z. Hu, J.H. Kwak, Z. Yang, X. Wan, and L. Shaw, "Direct observation of ion exchange in mechanically activated LiH+MgB_2 system using ultra-high field nuclear magnetic resonance spectroscopy," Appl. Phys. Lett., 94, 141905 (2009).

8. H.B. Borgstedt and C. Guminski, "The B-Li (boron-lithium) system," J. Phase Equilibria, 24, 572 (2003).

9. Z.J. Liu, X.H. Qu, and B.Y. Huang, "XRD intensity calculation and electron density function of LiB compound," Acta Metall. Sinica., 37, 340 (2001).

10. A.N. Kolmogorov and S. Stefano Curtarolo, "Theoretical study of metal borides stability," Phys. Rev. B, 74, 224507 (2006).

11. J. Kostka, W. Lohstroh, M. Fichtner, and H. Hahn, "Diborane release from $LiBH_4$/silica-gel mixtures and the effect of additives," J. Phys. Chem. C, 111, 14026 (2007).